


Space-charge-limited current density for nonplanar diodes with monoenergetic emission using Lie-point symmetries

N. R. Sree Harsha¹, Jacob M. Halpern¹, Adam M. Darr^{1,*} and Allen L. Garner^{1,2,3,†}

¹*School of Nuclear Engineering, Purdue University, West Lafayette, Indiana 47906, USA*

²*Elmore Family School of Electrical and Computer Engineering, Purdue University, West Lafayette, Indiana 47907, USA*

³*Department of Agricultural and Biological Engineering, Purdue University, West Lafayette, Indiana 47907, USA*

 (Received 14 March 2022; revised 15 November 2022; accepted 1 December 2022; published 26 December 2022)

Understanding space-charge-limited current density (SCLCD) is fundamentally and practically important for characterizing many high-power and high-current vacuum devices. Despite this, no analytic equations for SCLCD with nonzero monoenergetic initial velocity have been derived for nonplanar diodes from first principles. Obtaining analytic equations for SCLCD for nonplanar geometries is often complicated by the nonlinearity of the problem and over constrained boundary conditions. In this Letter, we use the canonical coordinates obtained by identifying Lie-point symmetries to linearize the governing differential equations to derive SCLCD for any orthogonal diode. Using this method, we derive exact analytic equations for SCLCD with a monoenergetic injection velocity for one-dimensional cylindrical, spherical, tip-to-tip (t-t), and tip-to-plate (t-p) diodes. We specifically demonstrate that the correction factor from zero initial velocity to monoenergetic emission depends only on the initial kinetic and electric potential energies and not on the diode geometry and that SCLCD is universal when plotted as a function of the canonical gap size. We also show that SCLCD for a t-p diode is a factor of four larger than a t-t diode independent of injection velocity. The results reduce to previously derived results for zero initial velocity using variational calculus and conformal mapping.

DOI: [10.1103/PhysRevE.106.L063201](https://doi.org/10.1103/PhysRevE.106.L063201)

Ordinary differential equations (ODEs) and partial differential equations (PDEs) are used extensively to model the behavior of many systems in applied physics and mathematics [1], including tumor growth [2,3], heat transfer [4,5], fluid mechanics [6], neutron transport [7], chemical engineering [8], electromagnetism [9], and electroporation [10–12]. Consider the general first-order ODE of the form

$$\frac{dy}{dx} = f(x, y), \quad (1)$$

where $f(x, y)$ is a smooth function of x and y . If function f in (1) is a function of x alone [i.e., $f(x, y) \equiv f(x)$], we can readily solve (1) by quadrature,

$$y = \int f(x)dx + c \quad (2)$$

for some integration constant c . If, however, $f(x, y)$ in (1) cannot be separated into a product of two functions such that $f(x, y) = g(x)h(y)$ for some smooth functions g and h , the solution to the ODE cannot be obtained directly by quadrature. This often arises for the applications described above [1–12], particularly, for complicated geometries. For such situations, we can use the Lie-point symmetries of (1) to identify a set of canonical coordinates that reduces (1) to a form that can

be solved directly by quadrature (2) [13–15]. These canonical coordinates represent local transformations that map every solution set of a system to another solution set of the same system for which known solutions exist or can be obtained directly by quadrature. Similar transformations can be applied to simplify and solve higher-order ODEs and PDEs.

We demonstrate this approach in this Letter by solving a second-order ODE to derive exact analytic solutions for space-charge limited current density (SCLCD) in vacuum with nonzero monoenergetic electron injection velocity in any orthogonal diode geometry. The SCLCD is the maximum steady-state current density that can flow between a cathode and an anode in vacuum [16,17]. Characterizing SCLCD is critical for numerous applications, including electric propulsion, nanovacuum transistors, thermionic energy converters, solar power conversion, high-power microwaves, and microplasma formation [16,17]. For a one-dimensional (1D) planar diode, the exact analytic equation for classical nonrelativistic SCLCD, first derived by Child and Langmuir (CL) [18,19], is given by

$$J_{\text{CL}} = \frac{\gamma V_g^{3/2}}{(x_A - x_C)^2}, \quad (3)$$

where $\gamma = 4\epsilon_0\sqrt{2e/m}/9$, ϵ_0 is the permittivity of vacuum, e and m are the charge and mass of the electron, respectively, the anode is held at a constant voltage V_g located at $x = x_A$, and the grounded cathode is located at $x = x_C$. Various studies have extended the CL law to account for multiple dimensions [20–27], nonplanar diode geometries [28–34],

*Present Address: Sandia National Laboratories, Albuquerque, NM 87123, USA.

†Author to whom any correspondence should be addressed: algarner@purdue.edu

time-varying voltages [35–38], bipolar flow [39–42], relativistic effects [43,44], trap-filled solids [45–47], and quantum effects [48–51].

When the electron injection velocity is zero, the electron charge density is infinite at the cathode, and the corresponding SCLCD, given by (3), can only be obtained as the limit of an indeterminate 0/0 singularity at the cathode [52]. Jaffé avoided this singularity by deriving SCLCD for a constant nonzero electron injection velocity and recovered (3) by taking the limit as the ratio of the kinetic energy to the electric potential energy approached zero [53]. Recently, Lafleur [54] validated Jaffé's results using particle-in-cell simulations, and Huang *et al.* [55] used a sheet model to simulate the injection of electrons with either a monoenergetic or a Maxwell-Boltzmann velocity distribution. In this Letter, we extend (3) to include a constant nonzero initial velocity in a 1D planar geometry before further generalizing SCLCD to *any* 1D diode geometry represented by an orthogonal coordinate system, which we use to derive SCLCD for cylindrical, spherical, tip-to-tip, and tip-to-plate geometries. We only consider 1D analysis and ignore image charges.

We first consider a 1D planar diode with cathode and anode, represented by infinite planes, located at $x = x_C$ and $x = x_A$, respectively. The anode is held at a constant potential V_g , whereas, the cathode is grounded. Continuity implies that the local current density in planar coordinates is $J_p = \rho_p v_p$, where ρ_p is the charge density and v_p is the electron velocity across the gap. From conservation of energy in 1D flow, given by $mv_p^2/2 = mv_0^2/2 + e\phi_p$ [54], we obtain

$$v_p = v_0 \sqrt{1 + \frac{2e\phi_p}{mv_0^2}}, \quad (4)$$

where ϕ_p is the electric potential in the planar gap and v_0 is the electron velocity at the cathode. Including nonzero v_0 avoids the 0/0 singularity in J_p and infinite ρ_p at the cathode and elucidates virtual cathode behavior in various orthogonal geometries [53,54]. Considering variation only in the x direction, Poisson's equation in planar coordinates is given by

$$\frac{d^2\phi_p}{dx^2} = \frac{\rho_p}{\epsilon_0} = \frac{J_p}{\epsilon_0 v_p}. \quad (5)$$

Combining (4) and (5), we obtain

$$J_p = \epsilon_0 v_0 \frac{d^2\phi_p}{dx^2} \sqrt{1 + \frac{2e\phi_p}{mv_0^2}}. \quad (6)$$

The planar SCLCD at the cathode $J_{p,\text{SCL}}$ is given by

$$J_{p,\text{SCL}} = \lim_{x \rightarrow x_C} [\max(J_p)] = \max[\lim_{x \rightarrow x_C} (J_p)], \quad (7)$$

where we define $\max(\cdot)$ as a continuous functional that takes the expression on the right-hand side of (6) as an input and generates the maximum value of J_p (denoted as $J_{p,\text{SCL}}$) as the output. We will now present a general definition and derivation of the $\max(\cdot)$ functional.

Derivation of $\max(\cdot)$. For generality, we consider the current density J in general canonical coordinates ζ . We consider all current and electron velocity to be in the ζ direction.

Writing (6) in canonical coordinates gives

$$J = \epsilon_0 v_0 \frac{d^2\phi_\zeta}{d\zeta^2} \sqrt{1 + \frac{2e\phi_\zeta}{mv_0^2}}, \quad (8)$$

with the grounded cathode at $\zeta = \zeta_C$ and the anode biased to V_g at $\zeta = \zeta_A$. To simplify the derivation, we define $v_D^2 = 2eV_g/m$ and the following dimensionless parameters [54]:

$$\bar{\phi}_\zeta = \frac{\phi_\zeta}{V_g}, \quad \bar{\zeta} = \frac{\zeta - \zeta_C}{\zeta_A - \zeta_C}, \quad \beta^2 = \frac{mv_0^2}{2eV_g},$$

$$\bar{J} = \frac{J_{\text{SCL}}(\zeta_A - \zeta_C)^2}{\epsilon_0 V_g v_D}. \quad (9)$$

Rewriting (8) in terms of the dimensionless parameters from (9), we obtain

$$\bar{J} = \frac{d^2\bar{\phi}_\zeta}{d\bar{\zeta}^2} \sqrt{\bar{\phi}_\zeta + \beta^2}. \quad (10)$$

Multiplying both sides of (10) by $d\bar{\phi}/d\bar{\zeta}$ and simplifying yields

$$\frac{1}{2} \frac{d}{d\bar{\zeta}} \left(\frac{d\bar{\phi}_\zeta}{d\bar{\zeta}} \right)^2 = \frac{\bar{J}}{\sqrt{\beta^2 + \bar{\phi}_\zeta}} \left(\frac{d\bar{\phi}_\zeta}{d\bar{\zeta}} \right). \quad (11)$$

Multiplying both sides of (11) by $d\bar{\zeta}$ and integrating gives a modified version of Poisson's Eq. (5) as

$$\frac{1}{2} \int_0^{\bar{\zeta}} d \left(\frac{d\bar{\phi}_\zeta}{d\bar{\zeta}} \right)^2 = \bar{J} \int_0^{\bar{\phi}_\zeta} \frac{d\bar{\phi}_\zeta}{\sqrt{\beta^2 + \bar{\phi}_\zeta}}. \quad (12)$$

Simplifying (12), we obtain

$$\left(\frac{d\bar{\phi}_\zeta}{d\bar{\zeta}} \right)^2 = \left(\frac{d\bar{\phi}_\zeta}{d\bar{\zeta}} \right)^2 \Big|_{\bar{\zeta}=0} + 4\bar{J}(\sqrt{\beta^2 + \bar{\phi}_\zeta} - \beta). \quad (13)$$

Letting $\bar{\zeta}^*$ denote the location of the virtual cathode where the electric field goes to zero, and $\bar{\phi}_\zeta^*$ denote the potential at $\bar{\zeta}^*$ gives

$$\left(\frac{d\bar{\phi}}{d\bar{\zeta}} \right)^2 \Big|_{\bar{\zeta}=0} = -4\bar{J}(\sqrt{\beta^2 + \bar{\phi}_\zeta^*} - \beta). \quad (14)$$

Substituting (14) into (13) and simplifying yields

$$\frac{d\bar{\phi}_\zeta}{d\bar{\zeta}} = \pm 2\sqrt{\bar{J}}(\sqrt{\beta^2 + \bar{\phi}_\zeta} - \sqrt{\beta^2 + \bar{\phi}_\zeta^*})^{1/2}. \quad (15)$$

The normalized electric field, defined as $\bar{E} = -d\bar{\phi}_\zeta/d\bar{\zeta}$, is positive for $0 \leq \bar{\zeta} \leq \bar{\zeta}^*$ and negative for $\bar{\zeta}^* \leq \bar{\zeta} \leq 1$, whereas the electric field is zero at $\bar{\zeta} = \bar{\zeta}^*$. Integrating (15) while accounting for this sign change gives

$$-\int_0^{\bar{\phi}_\zeta^*} \frac{d\bar{\phi}_\zeta}{(\sqrt{\beta^2 + \bar{\phi}_\zeta} - \sqrt{\beta^2 + \bar{\phi}_\zeta^*})^{1/2}} + \int_{\bar{\phi}_\zeta^*}^1 \frac{d\bar{\phi}_\zeta}{(\sqrt{\beta^2 + \bar{\phi}_\zeta} - \sqrt{\beta^2 + \bar{\phi}_\zeta^*})^{1/2}} = 2\sqrt{\bar{J}} \int_0^1 d\bar{\zeta}. \quad (16)$$

Defining $\eta_L = \sqrt{\beta^2 + 1}$ and $\eta^* = \sqrt{\beta^2 + \bar{\phi}_\zeta^*}$ allows to rewrite (16) as

$$\sqrt{\bar{J}} = \frac{2}{3}(\beta - \eta^*)^{1/2}(\beta + 2\eta^*) + \frac{2}{3}(\eta_L - \eta^*)^{1/2}(\eta_L + 2\eta^*). \quad (17)$$

We can find the extremum of \bar{J} by setting $d\sqrt{\bar{J}}/d\eta^* = 0$ in (17), yielding $\eta_{\max}^* = \beta\eta_L/(\beta + \eta_L)$ [54]. Evaluating (17) at $\eta^* = \eta_{\max}^*$ gives the maximum stable current density in dimensionless parameters as

$$\bar{J}_{\text{SCL}} = \frac{4}{9}(\beta + \sqrt{1 + \beta^2})^3. \quad (18)$$

Redimensionalizing (18) using (9) yields

$$J_{\text{SCL}} = \frac{\gamma V_g^{3/2}}{(\zeta_A - \zeta_C)^2}(\beta + \sqrt{1 + \beta^2})^3. \quad (19)$$

Hence, we define the $\max(\cdot)$ operator for canonical coordinates from (8) and (19) as

$$\max \left[\epsilon_0 v_0 \frac{d^2 \phi_\zeta}{d\zeta^2} \sqrt{1 + \frac{2e\phi_\zeta}{mv_0^2}} \right] = \frac{\gamma V_g^{3/2}}{(\zeta_A - \zeta_C)^2}(\beta + \sqrt{1 + \beta^2})^3. \quad (20)$$

Note that SCLCD, which may depend on position when written in orthogonal coordinates, is constant when written in canonical coordinates for any given diode.

We next apply this definition for a few orthogonal diode geometries. For the 1D planar problem, we substitute J_p from (6) into (7) to obtain the SCLCD as

$$J_{p,\text{SCL}} = (\beta + \sqrt{1 + \beta^2})^3 J_{\text{CL}}. \quad (21)$$

Poisson's Eq. (12) is separable in Cartesian coordinates since the spatial dependence can be isolated; however, this is not true for nonplanar diode geometries since the Laplacian in Poisson's equation becomes nonlinear. For such nonlinear ODEs, we can introduce canonical coordinates to make them separable and derive analytical equations for SCLCD. To illustrate this approach, we first derive SCLCD in general orthogonal coordinates. We then consider 1D concentric cylindrical, concentric spherical, tip-to-tip (t-t), and tip-to-plate (t-p) geometries.

General coordinates. We now derive analytic equations for SCLCD in any orthogonal geometry by considering the generalized metric $ds^2 = (h_1 dq_1)^2 + (h_2 dq_2)^2 + (h_3 dq_3)^2 = \sum (h_i dq_i)^2$, where ds represents the infinitesimal distance between any two points, and q_i and h_i represent the orthogonal coordinates and scaling factors, respectively [56]. We will only consider a 1D diode geometry where the potential ϕ_q varies only with q_1 . The anode and cathode are at q_A and q_C , respectively. Continuity requires that the local current density $J_q = \rho_q v_q$, where ρ_q and v_q represent the electron charge density and velocity in the gap in the q_1 direction. We may write Poisson's equation as [57]

$$\frac{1}{h_1 h_2 h_3} \frac{d}{dq_1} \left(\frac{h_2 h_3}{h_1} \frac{d\phi_q}{dq_1} \right) = \frac{J_q}{\epsilon_0 v_q}. \quad (22)$$

Using conservation of energy for 1D flow in general coordinates, given by $mv_q^2/2 = mv_0^2/2 + e\phi_q$, allows us to write

(22) as

$$J_q = \epsilon_0 v_0 \left[\frac{1}{h_1 h_2 h_3} \frac{d}{dq_1} \left(\frac{h_2 h_3}{h_1} \frac{d\phi_q}{dq_1} \right) \right] \sqrt{1 + \frac{2e\phi_q}{mv_0^2}}, \quad (23)$$

where v_0 represents the velocity of the electrons at the cathode in the q_1 direction. To make (23) separable, we introduce the canonical coordinate ζ_q such that $d\zeta_q/dq_1 = h_1/(h_2 h_3)$. Using the canonical coordinate ζ_q , defining $\phi_q[\zeta_q(q_1)] \equiv \phi_{\zeta_q}$, and applying the chain rule allows us to recast (23) as

$$J_q = \epsilon_0 v_0 \left[\frac{1}{(h_2 h_3)^2} \left(\frac{d^2 \phi_{\zeta_q}}{d\zeta_q^2} \right) \right] \sqrt{1 + \frac{2e\phi_{\zeta_q}}{mv_0^2}}. \quad (24)$$

SCLCD $J_{q,\text{SCL}}$, which corresponds to the maximum current density emitted from the cathode, is defined as [assuming that $\max(\cdot)$ is continuous everywhere],

$$\lim_{q \rightarrow q_C} \{ \max [(h_2 h_3)^2 J_q] \} = \max \left\{ \lim_{q \rightarrow q_C} [(h_2 h_3)^2 J_q] \right\} = J_{q,\text{SCL}} [(h_2 h_3)^2 |_{q=q_C}]. \quad (25)$$

We may then write SCLCD by substituting (24) into (25) to obtain

$$J_{q,\text{SCL}} = \frac{\epsilon_0 v_0}{(h_2 h_3)^2 |_{q=q_C}} \max \left[\left(\frac{d^2 \phi_{\zeta_q}}{d\zeta_q^2} \right) \sqrt{1 + \frac{2e\phi_{\zeta_q}}{mv_0^2}} \right]. \quad (26)$$

One of the requirements for writing Poisson's equation for a system is $\nabla \times \mathbf{E} = 0$, which implies $\mathbf{E} = -\nabla\phi$. However, any curl equation, such as $\nabla \times \mathbf{E} = 0$, is a three-dimensional (3D) equation that only makes sense in three dimensions of space. Hence, current densities obtained from Poisson's equation are equations in three-dimensional space, which can also be observed by noting that Poisson's equation *always* yields current densities with units of A/m² in *any number* of dimensions. Accounting for continuity in one direction differs between 1D and 3D systems since the units of current density must be preserved due to Poisson's equation. In 1D, the current density should have units of A because the other two dimensions do not exist. Hence, J must be multiplied by the corresponding orthogonal coordinates in the continuity equation when truly in 1D to convert from A/m² to A. In 3D, the standard divergence accounts for the full geometry. Hence, we note that continuity for 1D flow, in general, orthogonal coordinates is given by $\nabla \cdot (\chi \vec{J}_q) = 0$, where $\chi = h_2 h_3$ for a flow in 1D (along q_1), $\chi = h_3$ for a flow in two dimensions (e.g., on the $q_1 q_2$ plane), and $\chi = 1$ for a flow in three dimensions [58]. For a flow in q_1 , the continuity equation reduces to $d(h_2 h_3^2 J_q)/dq_1 = 0$. Furthermore, noting that the argument of $\max(\cdot)$ in (26) exactly equals the argument defined in (20) and substituting $\zeta_{q,A} = [\int h_1 dq/(h_2 h_3)]|_{q=q_A}$, and $\zeta_{q,C} = [\int h_1 dq/(h_2 h_3)]|_{q=q_C}$ gives SCLCD at the cathode in the general orthogonal coordinate system as

$$J_{q,\text{SCL}} = \frac{(h_2 h_3)^{-2} |_{q=q_C} \gamma V_g^{3/2} (\beta + \sqrt{1 + \beta^2})^3}{\left([\int \frac{h_1 dq}{h_2 h_3}] |_{q=q_A} - [\int \frac{h_1 dq}{h_2 h_3}] |_{q=q_C} \right)^2}. \quad (27)$$

Equation (27) represents the general form of the SCLCD by using the definition of metric ds^2 alone without having to solve the nonlinear Poisson's equation. Equation (27) is true

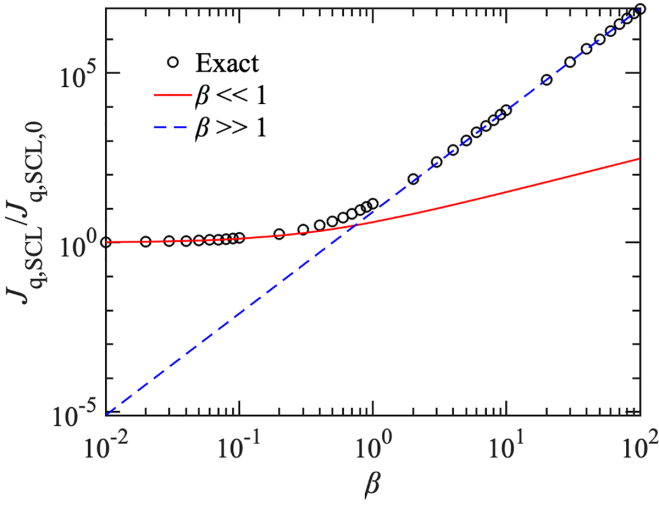


FIG. 1. The exact solution of the ratio of SCLCD in general coordinates to the corresponding SCLCD with zero injection velocity in general coordinates as a function of β from (28) with limits for $\beta \ll 1$ from (30) and $\beta \gg 1$ from (31).

for any orthogonal geometry. We may then write SCLCD in general orthogonal coordinates as

$$\frac{J_{q,SCL}}{J_{q,SCL,0}} = (\beta + \sqrt{1 + \beta^2})^3, \quad (28)$$

where SCLCD with $v_0 = 0$, $J_{q,SCL,0}$ (i.e., $\beta = 0$), is given by

$$J_{q,SCL,0} = \frac{(h_2 h_3)^{-2} |_{q=q_C} \gamma V_g^{3/2}}{\left(\left[\int \frac{h_1 dq}{h_2 h_3} \right] |_{q=q_A} - \left[\int \frac{h_1 dq}{h_2 h_3} \right] |_{q=q_C} \right)^2}. \quad (29)$$

For $\beta \ll 1$, we approximate (28) as

$$\frac{J_{q,SCL}}{J_{q,SCL,0}} \approx 1 + 3\beta. \quad (30)$$

For $\beta \gg 1$, we approximate (28) as

$$\frac{J_{q,SCL}}{J_{q,SCL,0}} \approx 8\beta^3. \quad (31)$$

Figure 1 shows $J_{q,SCL}/J_{q,SCL,0}$ as a function of β for the exact (29) and asymptotic [(30), (31)] solutions. We next apply this approach to common orthogonal coordinate systems and show how continuity is satisfied in each case.

Example 1. We first consider a concentric 1D cylindrical diode in polar coordinates with the cathode at $r = r_C$ and the anode at $r = r_A$. Using the metric $ds^2 = dr^2 + r^2 d\theta^2 + dz^2$ in polar cylindrical coordinates gives Poisson's equation for variation only in the r direction as

$$\frac{1}{r} \frac{d}{dr} \left(r \frac{d\phi_c}{dr} \right) = \frac{J_c}{\epsilon_0 v_c}, \quad (32)$$

where the local current density in cylindrical coordinates is given by $J_c = \rho_c v_c$, where ρ_c and v_c represent charge density and electron velocity in cylindrical coordinates. To make (32) separable, we define a canonical coordinate ζ_c that reduces (32) to a separable form [59]. Upon inspection, we may define ζ_c such that $d\zeta_c/dr = 1/r$, which yields $\zeta_c = \ln r$ and reduces

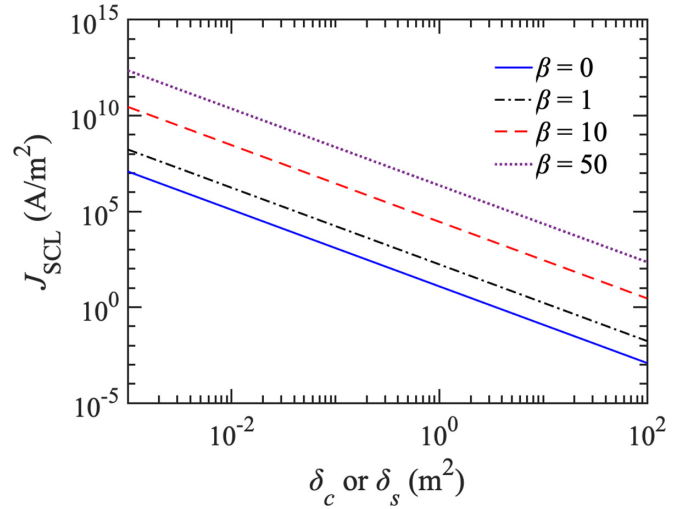


FIG. 2. SCLCD (J_{SCL}) as a function of canonical gap size $\delta_c = r_C^2 [\ln(r_C/r_A)]^2$ or $\delta_s = r_C^2 [r_A - r_C]^2/r_A^2$ for cylindrical or spherical coordinates, respectively, for various values of β . The applied voltage is $V_g = 30$ kV. Note that J_{SCL} is the same for any geometry for a given canonical gap size.

(32) to

$$J_c = \frac{\epsilon_0 v_0}{r^2} \left(\frac{d^2 \phi_{\zeta_c}}{d\zeta_c^2} \right) \sqrt{1 + \frac{2e\phi_{\zeta_c}}{mv_0^2}}, \quad (33)$$

where $\phi_c[\zeta_c(r)] \equiv \phi_{\zeta_c}$. Assuming that $\max(\cdot)$ is continuous everywhere, the maximum current density (SCLCD) at the cathode is

$$\lim_{r \rightarrow r_C} [\max(r^2 J_c)] = \max \left[\lim_{r \rightarrow r_C} (r^2 J_c) \right] = r_C^2 J_{c,SCL}. \quad (34)$$

Substituting (33) into (34) yields

$$r_C^2 J_{c,SCL} = \epsilon_0 v_0 \max \left[\left(\frac{d^2 \phi_{\zeta_c}}{d\zeta_c^2} \right) \sqrt{1 + \frac{2e\phi_{\zeta_c}}{mv_0^2}} \right]. \quad (35)$$

Applying (20) in (35) and noting that $\zeta_{c,A} = \ln r_A$ and $\zeta_{c,C} = \ln r_C$, we obtain

$$J_{c,SCL} = \frac{\gamma V_g^{3/2}}{r_C^2 (\ln r_A - \ln r_C)^2} (\beta + \sqrt{1 + \beta^2})^3. \quad (36)$$

For $v_0 = 0$ ($\beta = 0$), (36) reduces to $J_{c,SCL} = \gamma V_g^{3/2} / [r_C^2 (\ln r_A - \ln r_C)^2]$, which agrees with the result from variational calculus (VC) [30] and conformal mapping (CM) [31]. Continuity is satisfied in (36) since it requires that $d(r^2 J_c)/dr = 0$ [58,60] for 1D flow in cylindrical coordinates. Note that this derivation is completely independent of the VC and CM techniques and was obtained without using the 1D continuity definition. Figure 2 shows $J_{c,SCL}$ as a function of the canonical gap size $\delta_c = r_C^2 [\ln(r_C/r_A)]^2$ for various values of β .

Example 2. We next consider a concentric 1D spherical diode with the anode and cathode located at r_A and r_C , respectively. Defining $ds^2 = dr^2 + r^2 d\phi^2 + r^2 \sin^2 \phi d\theta^2$ as the metric and assuming variation only in the r direction gives

Poisson's equation as

$$\frac{1}{r^2} \frac{d}{dr} \left(r^2 \frac{d\phi_s}{dr} \right) = \frac{J_s}{\epsilon_0 v_s}, \quad (37)$$

with local current density $J_s = \rho_s v_s$. We define the canonical coordinate ζ_s such that $d\zeta_s/dr = 1/r^2$, yielding $\zeta_s = -1/r$. Rewriting (37) in terms of canonical coordinates and defining $\phi_s[\zeta_s(r)] \equiv \phi_{\zeta_s}$ gives

$$J_s = \frac{\epsilon_0 v_0}{r^4} \left(\frac{d^2 \phi_{\zeta_s}}{d\zeta_s^2} \right) \sqrt{1 + \frac{2e\phi_{\zeta_s}}{mv_0^2}}. \quad (38)$$

Assuming that $\max(\cdot)$ is continuous everywhere, SCLCD at the cathode can be obtained by

$$\lim_{r \rightarrow r_C} [\max(r^4 J_s)] = \max \left[\lim_{r \rightarrow r_C} (r^4 J_s) \right] = r_C^4 J_{s,\text{SCL}}. \quad (39)$$

Using (39) to maximize (38) yields

$$r_C^4 J_{s,\text{SCL}} = \epsilon_0 v_0 \max \left[\left(\frac{d^2 \phi_{\zeta_s}}{d\zeta_s^2} \right) \sqrt{1 + \frac{2e\phi_{\zeta_s}}{mv_0^2}} \right]. \quad (40)$$

Using (20) in (40) and noting that $\zeta_{s,A} = -1/r_A$ and $\zeta_{s,C} = -1/r_C$, we obtain

$$J_{s,\text{SCL}} = \frac{\gamma V_g^{3/2} r_A^2}{r_C^2 (r_A - r_C)^2} (\beta + \sqrt{1 + \beta^2})^3. \quad (41)$$

For $v_0 = 0$ (i.e., $\beta = 0$), (41) reduces to $J_{s,\text{SCL}} = \gamma V_g^{3/2} r_A^2 / [r_C^2 (r_A - r_C)^2]$, which agrees with VC [30] and provides an independent verification of this approach. Continuity for 1D flow in spherical coordinates, given by $d(r^4 J_s)/dr = 0$ [58,60], is satisfied in (41). Figure 2 shows $J_{s,\text{SCL}}$ as a function of the canonical gap size $\delta_s = r_C^2 [r_A - r_C]^2 / r_A^2$ for various values of β . SCLCD is independent of geometry when plotted as a function of the canonical gap size, so this plot may be used for *any* geometry and converted to physical dimensions by using the appropriate metric.

Example 3. We next consider t-t and t-p geometries where the cathode and the anode are represented by hyperboloids η_C and η_A , respectively, in prolate spheroidal coordinates [32]. The prolate spheroidal coordinate system models a 1D infinite hyperbolic cathode and anode facing each other, with $\eta = \pi/2$ modeling the t-p geometry (cf. Fig. 1 of Ref. [32]). The surfaces of constant η , given by $z^2/\cos^2(\eta) - (x^2 + y^2)/\sin^2(\eta) = a^2$, represent the hyperboloid of revolution [32]. Although prolate spheroidal coordinates are a natural orthogonal coordinate system to study the SCLCD for a tip, the radius of curvature is fixed for each hyperboloid tip. We can compensate for this restriction by choosing an appropriate distance between the foci of the hyperboloids, which is given by $a/2$, to model a given experimental setup [32]. The metric in prolate spheroidal coordinates is given by $ds^2 = a^2[(\sinh^2 \xi + \sin^2 \eta)(d\xi^2 + d\eta^2) + (\sinh^2 \xi \sin^2 \eta)d\varphi^2]$. If J_{t-t} represents the local current density in the t-t geometry, Poisson's equation, assuming variation only in the η direction, is given by [32]

$$\frac{1}{a^2} \frac{1}{(\sinh^2 \xi + \sin^2 \eta) \sin \eta} \frac{d}{d\eta} \left(\sin \eta \frac{d\phi_\eta}{d\eta} \right) = \frac{J_{t-t}}{\epsilon_0 v_\eta}. \quad (42)$$

Using conservation of energy, given by $mv_\eta^2/2 = mv_0^2/2 + e\phi_\eta$, and defining the canonical coordinate ζ_t such that $d\zeta_t/d\eta = 1/\sin \eta$ and $\phi_\eta[\zeta_t(\eta)] \equiv \phi_{\zeta_t}$, reduces (42) to

$$J_{t-t} = \frac{\epsilon_0 v_0}{a^2 (\sinh^2 \xi + \sin^2 \eta) \sin^2 \eta} \left(\frac{d^2 \phi_{\zeta_t}}{d\zeta_t^2} \right) \sqrt{1 + \frac{2e\phi_{\zeta_t}}{mv_0^2}}. \quad (43)$$

Assuming that $\max(\cdot)$ is continuous everywhere, SCLCD at the cathode tip can be written as

$$\begin{aligned} \lim_{\eta \rightarrow \eta_C} [\max(a^2 \sin^4 \eta J_{t-t})] &= \max \left[\lim_{\eta \rightarrow \eta_C} (a^2 \sin^4 \eta J_{t-t}) \right] \\ &= J_{t-t,\text{SCL}} a^2 \sin^4 \eta_C. \end{aligned} \quad (44)$$

Substituting (43) into (44) and noting that $\sinh \xi = 0$ at the cathode tip yields

$$J_{t-t,\text{SCL}} a^2 \sin^4 \eta_C = \epsilon_0 v_0 \max \left[\left(\frac{d^2 \phi_{\zeta_t}}{d\zeta_t^2} \right) \sqrt{1 + \frac{2e\phi_{\zeta_t}}{mv_0^2}} \right]. \quad (45)$$

Using (20) in (45) and noting that $\zeta_{t,A} = \ln[\tan(\eta_A/2)]$ and $\zeta_{t,C} = \ln[\tan(\eta_C/2)]$ gives SCLCD in t-t geometry at the cathode tip as

$$\begin{aligned} J_{t-t,\text{SCL}} &= \frac{\gamma V_g^{3/2}}{a^2 \sin^4 \eta_C (\ln[\tan(\frac{\eta_A}{2})] - \ln[\tan(\frac{\eta_C}{2})])^2} \\ &\quad \times (\beta + \sqrt{1 + \beta^2})^3. \end{aligned} \quad (46)$$

For $v_0 = 0$ ($\beta = 0$), (46) reduces to $J_{t-t,\text{SCL}} = \gamma V_g^{3/2} a^{-2} \sin^{-4} \eta_C \{ \ln[\tan(\eta_A/2)] - \ln[\tan(\eta_C/2)] \}^{-2}$, which agrees with VC and CM [32]. Continuity for 1D flow in prolate spheroidal coordinates requires that $d(h_2^2 h_3^2 J_{t-t})/d\eta = d[(\sinh^2 \xi + \sin^2 \eta) \sin^2 \eta J_{t-t}]/d\eta = 0$, where $h_2^2 = a^2 (\sinh^2 \xi + \sin^2 \eta)$ and $h_3^2 = a^2 \sinh^2 \xi \sin^2 \eta$ [58]. At the tip of the cathode represented by $\xi = 0$, $\sinh \xi = 0$ and the continuity equation reduces to $d(a^2 \sin^4 \eta J_{t-t})/d\eta = 0$; hence, continuity is satisfied in (46).

Assuming identical tips (i.e., $\eta_A = \pi - \eta_C$) and defining the distance between the apex of the tips as D_0 gives $a^2 = D_0(D_0 + R)$, where R is the radius of the tips [32]. Next, defining $\mu = D_0/R = \cot^2 \eta_A = \cot^2 \eta_C$ yields $\cos^2(\eta_A) = \cos^2(\eta_C) = D_0/(D_0 + R)$ and $\sin^4 \eta_C = \sin^4 \eta_A = R^2(D_0 + R)^{-2}$. Using these definitions and noting that $x_A - x_C = D_0$ gives (46) in terms of J_{CL} with $D_0^2 = (x_A - x_C)^2$ as

$$\frac{J_{t-t,\text{SCL}}}{J_{\text{CL}}} = \frac{\mu(\mu + 1)}{4[\ln(\sqrt{1 + \mu} + \sqrt{\mu})]^2} (\beta + \sqrt{1 + \beta^2})^3, \quad (47)$$

where we used $\sqrt{1 + \mu} - \sqrt{\mu} = (\sqrt{1 + \mu} + \sqrt{\mu})^{-1}$.

The SCLCD for t-p can be obtained from (46) by noting that the anode (a plate) is represented in prolate spheroidal coordinates with $\eta_A \rightarrow \pi/2$ in (46), which necessitates $\ln[\tan(\eta_A/2)] \rightarrow 0$ [32]. Applying this and $v_0 = 0$ to (46) gives $J_{t-p,\text{SCL}} = \gamma V_g^{3/2} a^{-2} \sin^{-4} \eta_C (\ln[\tan(\eta_C/2)])^{-2}$, which agrees with VC and CM [32]. Hence, SCLCD near the cathode tip in t-p geometry is given by

$$\frac{J_{t-p,\text{SCL}}}{J_{\text{CL}}} = \frac{\mu(\mu + 1)}{[\ln(\sqrt{1 + \mu} + \sqrt{\mu})]^2} (\beta + \sqrt{1 + \beta^2})^3. \quad (48)$$

Writing (47) and (48) in this form further shows that $J_{t-p,\text{SCL}} = 4J_{t-t,\text{SCL}}$, which was not apparent from the forms we

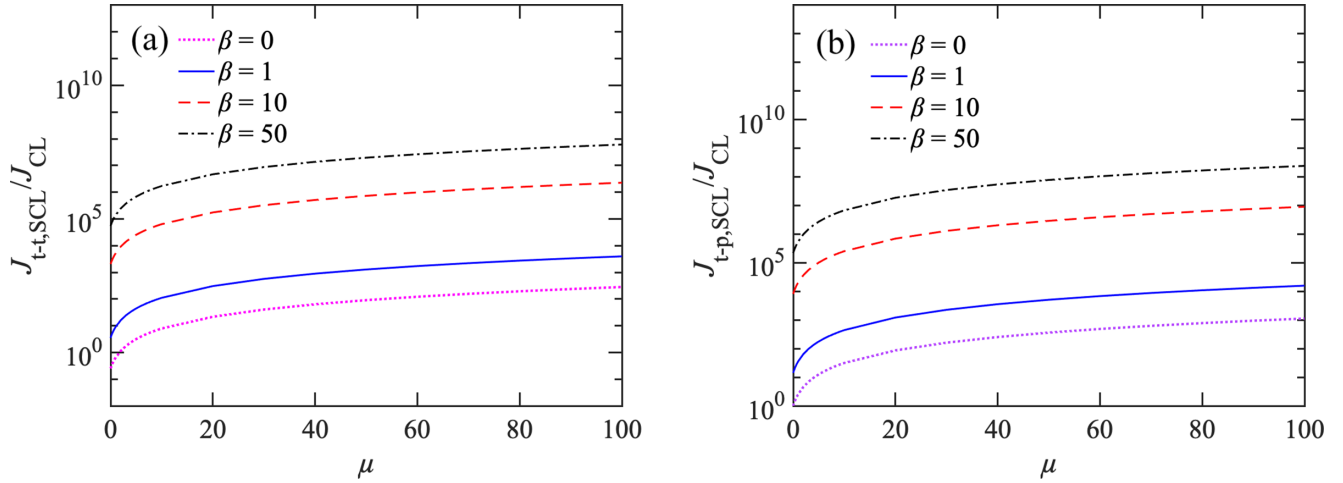


FIG. 3. SCLCD normalized to CL as a function of $\mu = D_0/R$ for various values of β for (a) tip-tip ($J_{t-t,SCL}/J_{CL}$) and (b) tip-to-plate ($J_{t-p,SCL}/J_{CL}$) geometries.

derived for $v_0 = 0$ using CM [32]. Figure 3 shows $J_{t-t,SCL}/J_{CL}$ and $J_{t-p,SCL}/J_{CL}$ as a function of μ for various values of β . Equations (47) and (48) show that SCLCD increases by $4\times$ as the anode tip becomes a horizontal plate for a given v_0 .

To summarize, we have demonstrated how to obtain canonical coordinates to make Poisson's equation separable to solve for SCLCD in general orthogonal coordinates for nonzero monoenergetic injection velocities and then for four simple geometries. Of particular note, we have provided independent validation of previous calculations of SCLCD using VC for cylindrical, spherical, tip-to-tip, and tip-to-plate geometries. We have also shown that the correction factor to account for initial velocity for any coordinate system is independent of geometry, so it is straightforward to write SCLCD for monoenergetic emission for a known 1D SCLCD with zero injection velocity. This may be valuable for complicated geometries that may not be amendable to this analysis, such as those we have studied previously using the CM [31]. We have also demonstrated that 1D SCLCD is independent of geometry once written as a function of canonical gap size (cf. Fig. 2); therefore, one may obtain SCLCD for a given geometry by applying the appropriate metric to the universal SCLCD. For ODEs and PDEs with nonobvious canonical coordinates, one may use Lie-point symmetries to derive the corresponding canonical coordinates to simplify the ODEs and PDEs [1,59]. This method provides various possible directions for future research. For instance, Lie-point symmetries may sim-

plify the governing PDEs in cylindrical crossed-field diode geometries [61].

Finally, we note that other current definitions [62,63] are claimed to be SCLCD for monoenergetic injection of electrons, but actually correspond to the bifurcation point in the diode [64]. SCLCD, as defined by the maximum current density permissible in the diode, is not related to the onset of reflection of particles but to the inherent nonlinear behavior of the governing ODEs [64]. We recently applied VC to simplify the Poisson's equation to delineate how the SCLCD and bifurcation point are obtained using the appropriate differential equations, boundary conditions, and functionals for extremization [65]. Future work will also apply these techniques to quantum [66], time-dependent [67], and relativistic conditions [44,68].

Data sharing is not applicable to this article as no new data were created or analyzed in this Letter.

This material is based upon work supported by the Air Force Office of Scientific Research under Awards No. FA9550-19-1-0101 and No. FA9550-22-1-0499. J.M.H. gratefully acknowledges funding from an Undergraduate Research Scholarship from the Purdue School of Nuclear Engineering. A.M.D. gratefully acknowledges funding from a Purdue Doctoral Fellowship. We also gratefully acknowledge L. K. Ang and J. Luginsland for useful discussions.

The authors have no conflict of interest to disclose.

[1] C. C. Lin and L. A. Segel, *Mathematics Applied to Deterministic Problems in Natural Sciences* (AM, Philadelphia, 1988).
 [2] Y. Kuang, J. D. Nagy, and S. E. Eikenberry, *Introduction to Mathematical Oncology* (CRC, Boca Raton, FL, 2016).
 [3] A. L. Garner, Y. Y. Lau, T. L. Jackson, M. D. Uhler, D. W. Jordan, and R. M. Gilgenbach, Incorporating spatial dependence into a multicellular tumor spheroid growth model, *J. Appl. Phys.* **98**, 124701 (2005).

[4] S. P. Venkateshan, *Heat Transfer*, 3rd ed. (Springer, Cham, 2020).
 [5] A. L. Garner, M. Deminksy, V. B. Neculaes, V. Chashihin, A. Knizhnik, and B. Potapkin, Cell membrane thermal gradients induced by electromagnetic fields, *J. Appl. Phys.* **113**, 214701 (2013).
 [6] P. K. Kundu, I. M. Cohen, and D. R. Dowling, *Fluid Mechanics*, 6th ed. (Elsevier, Oxford, 2016).

- [7] J. R. Lamarsh and A. J. Baratta, *Introduction to Nuclear Engineering*, 4th ed. (Pearson, Upper Saddle River, NJ, 2017).
- [8] C. G. Hill, Jr. and T. W. Root, *Introduction to Chemical Engineering Kinetics & Reactor Design*, 2nd ed. (Wiley, Hoboken, NJ, 2014).
- [9] J. D. Jackson, *Classical Electrodynamics*, 3rd ed. (Wiley, New York, 1999).
- [10] J. C. Weaver and Y. A. Chizmadzhev, Theory of electroporation: A review, *Bioelectrochem. Bioenerg.* **41**, 135 (1996).
- [11] C. Chen, S. W. Smye, M. P. Robinson, and J. A. Evans, Membrane electroporation theories: A review, *Med. Biol. Eng. Comput.* **44**, 5 (2006).
- [12] A. L. Garner and V. B. Neculaes, Extending membrane pore lifetime with AC fields: A modeling study, *J. Appl. Phys.* **112**, 014701 (2012).
- [13] P. E. Hydon, *Symmetry Methods for Differential Equations: A Beginner's Guide* (Cambridge University Press, Cambridge, UK, 2000).
- [14] B. Merkt, J. Timmer, and D. Kaschek, Higher-order Lie symmetries in identifiability and predictability analysis of dynamic models, *Phys. Rev. E* **92**, 012920 (2015).
- [15] F. Oliveri, Lie symmetries of differential equations: Classical results and recent contributions, *Symmetry* **2**, 658 (2010).
- [16] P. Zhang, Y. S. Ang, A. L. Garner, Á. Valfells, J. W. Luginsland, and L. K. Ang, Space-charge limited current in nanodiodes: Ballistic, collisional and dynamical effects, *J. Appl. Phys.* **129**, 100902 (2021).
- [17] P. Zhang, A. Valfells, L. K. Ang, J. W. Luginsland, and Y. Y. Lau, 100 years of the physics of the diodes, *Appl. Phys. Rev.* **4**, 011304 (2017).
- [18] C. D. Child, Discharge from hot CaO, *Phys. Rev. (Series 1)* **32**, 492 (1911).
- [19] I. Langmuir, The effect of space charge and residual gases on thermionic currents in high vacuum, *Phys. Rev.* **2**, 450 (1913).
- [20] Y. Y. Lau, Simple Theory for the Two-Dimensional Child-Langmuir Law, *Phys. Rev. Lett.* **87**, 278301 (2001).
- [21] J. W. Luginsland, Y. Y. Lau, R. J. Umstattd, and J. J. Watrous, Beyond the Child–Langmuir law: A review of recent results on multidimensional space-charge-limited flow, *Phys. Plasmas* **9**, 2371 (2002).
- [22] A. Rokhlenko and J. L. Lebowitz, Space-charge-limited 2d Electron Flow between Two Flat Electrodes in a Strong Magnetic Field, *Phys. Rev. Lett.* **91**, 085002 (2003).
- [23] A. Rokhlenko and J. L. Lebowitz, Space charge limited electron flow in two dimensions without magnetic field, *J. Appl. Phys.* **110**, 033306 (2011).
- [24] A. Rokhlenko and J. L. Lebowitz, Space charge limited two-dimensional electron flow in a rectangular geometry, *J. Appl. Phys.* **102**, 023305 (2007).
- [25] Y. B. Zhu and L. K. Ang, Non-uniform space charge limited current injection into a nano contact solid, *Sci. Rep.* **5**, 9173 (2015).
- [26] S. H. Chen, T. C. Tai, Y. L. Liu, L. K. Ang, and W. S. Koh, Two-dimensional electromagnetic Child–Langmuir law of a short-pulse electron flow, *Phys. Plasmas* **18**, 023105 (2011).
- [27] N. R. S. Harsha, M. Pearlman, J. Browning, and A. L. Garner, A multi-dimensional Child–Langmuir law for any diode geometry, *Phys. Plasmas* **28**, 122103 (2021).
- [28] I. Langmuir and K. Blodgett, Currents limited by space charge between coaxial cylinders, *Phys. Rev.* **22**, 347 (1923).
- [29] I. Langmuir and K. Blodgett, Currents limited by space charge between concentric spheres, *Phys. Rev.* **24**, 49 (1924).
- [30] A. M. Darr and A. L. Garner, A coordinate system invariant formulation for space-charge limited current in vacuum, *Appl. Phys. Lett.* **115**, 054101 (2019).
- [31] N. R. S. Harsha and A. L. Garner, Applying conformal mapping to derive analytical solutions of space-charge-limited current density for various geometries, *IEEE Trans. Electron Devices* **68**, 264 (2021).
- [32] N. R. S. Harsha and A. L. Garner, Analytic solutions for space-charge-limited current density from a sharp tip, *IEEE Trans. Electron Devices* **68**, 6525 (2021).
- [33] Y. B. Zhu and L. K. Ang, Space charge limited current emission for a sharp tip, *Phys. Plasmas* **22**, 052106 (2015).
- [34] A. L. Garner, A. M. Darr, and N. R. S. Harsha, A Tutorial on Calculating Space-Charge-Limited Current Density for General Geometries and Multiple Dimensions, *IEEE Trans. Plasma Sci.* **50**, 2528 (2022).
- [35] Y. N. Gartstein and P. Ramesh, Hysteresis and self-sustained oscillations in space charge limited currents, *J. Appl. Phys.* **83**, 2958 (1998).
- [36] M. Griswold, N. J. Fisch, and J. Wurtele, An upper bound to time-averaged space-charge limited diode currents, *Phys. Plasmas* **17**, 114503 (2010).
- [37] M. Griswold, N. J. Fisch, and J. Wurtele, Amended conjecture on an upper bound to time-dependent space-charge limited current, *Phys. Plasmas* **19**, 024502 (2012).
- [38] W. S. Koh, L. K. Ang, and T. J. Kwan, Multidimensional short-pulse space charge-limited flow, *Phys. Plasmas* **13**, 063102 (2006).
- [39] M. Y. Liao, R. H. Yao, and Y. B. Zhu, Space charge limited current for bipolar flow with uniform initial velocity, *Phys. Plasmas* **28**, 063508 (2021).
- [40] M. Y. Liao, R. H. Yao, and Y. B. Zhu, A numerical approach for space charge limited bipolar flow in cylindrical diodes, *IEEE J. Electron Devices* **9**, 1009 (2021).
- [41] Y. B. Zhu, M. Y. Liao, P. Zhao, and R. H. Yao, Nonuniform space charge limited current for 2-D bipolar flow in vacuum diode, *IEEE Trans. Electron Devices* **68**, 6538 (2021).
- [42] W. S. Koh, L. K. Ang, S. P. Lau, and T. J. T. Kwan, Space-charge limited bipolar flow in a nano-gap, *Appl. Phys. Lett.* **87**, 193112 (2005).
- [43] L. K. Ang and P. Zhang, Ultrashort-pulse Child-Langmuir Law in the Quantum and Relativistic Regimes, *Phys. Rev. Lett.* **98**, 164802 (2007).
- [44] A. D. Greenwood, J. F. Hammond, P. Zhang, and Y. Y. Lau, On relativistic space charge limited current in planar, cylindrical, and spherical diodes, *Phys. Plasmas* **23**, 072101 (2016).
- [45] W. Chandra, L. K. Ang, K. L. Pey, and C. M. Ng, Two-dimensional analytical Mott-Gurney law for a trap-filled solid, *Appl. Phys. Lett.* **90**, 153505 (2007).
- [46] Y. L. Liu, S. H. Chen, W. S. Koh, and L. K. Ang, Two-dimensional relativistic space charge limited current flow in the drift space, *Phys. Plasmas* **21**, 043101 (2014).
- [47] Y. B. Zhu, K. Geng, Z. S. Cheng, and R. H. Yao, Space-charge-limited current injection into free space and trap-filled solid, *IEEE Trans. Plasma Sci.* **49**, 2107 (2021).
- [48] Y. Y. Lau, D. Chernin, D. G. Colombant, and P.-T. Ho, Quantum Extension of Child-Langmuir Law, *Phys. Rev. Lett.* **66**, 1446 (1991).

- [49] L. K. Ang, T. J. T. Kwan, and Y. Y. Lau, New Scaling of Child–Langmuir Law in the Quantum Regime, *Phys. Rev. Lett.* **91**, 208303 (2003).
- [50] S. Bhattacharjee, A. Vartak, and V. Mukherjee, Experimental study of space-charge-limited flows in a nanogap, *Appl. Phys. Lett.* **92**, 191503 (2008).
- [51] D. Biswas and R. Kumar, The Child-Langmuir law in the quantum domain, *Europhys. Lett.* **102**, 58002 (2013).
- [52] R. J. Umstadtd, C. G. Carr, C. L. Frenzen, J. W. Luginsland, and Y. Y. Lau, A simple physical derivation of Child–Langmuir space-charge-limited emission using vacuum capacitance, *Am. J. Phys.* **73**, 160 (2005).
- [53] G. Jaffé, On the currents carried by electrons of uniform initial velocity, *Phys. Rev.* **65**, 91 (1944).
- [54] T. Lafleur, Space-charge limited current with a finite injection velocity revisited, *Plasma Sources Sci. Technol.* **29**, 065002 (2020).
- [55] J. B. Huang, R. H. Yao, P. Zhao, and Y. B. Zhu, Simulation of space-charge-limited current for hot electrons with initial velocity in a vacuum diode, *IEEE Trans. Electron Devices* **68**, 3604 (2021).
- [56] M. Vinokur, Conservation equations for gas dynamics in curvilinear coordinate systems, *J. Comput. Phys.* **14**, 105 (1974).
- [57] D. V. Redžić, The operator ∇ in orthogonal curvilinear coordinates, *Eur. J. Phys.* **22**, 595 (2001).
- [58] Z. Chen, G. Huan, and Y. Ma, *Computational Methods for Multiphase Flows in Porous Media* (SIAM, Philadelphia, PA, 2006), p. 12.
- [59] J. Starrett, Solving differential equations by symmetry groups, *Am. Math. Monthly* **114**, 778 (2007).
- [60] A. M. Darr, N. R. S. Harsha, and A. L. Garner, Response to “Comment on ‘A coordinate system invariant formulation for space-charge limited current in vacuum’” [*Appl. Phys. Lett.* **118**, 266101 (2021)], *Appl. Phys. Lett.* **118**, 266102 (2021).
- [61] A. M. Darr, R. Bhattacharya, J. Browning, and A. L. Garner, Space-charge limited current in planar and cylindrical crossed-field diodes using variational calculus, *Phys. Plasmas* **28**, 082110 (2021).
- [62] I. Langmuir, The effect of space charge and initial velocities on the potential distribution and thermionic current between parallel plane electrodes, *Phys. Rev.* **21**, 419 (1923).
- [63] S. Liu and R. A. Dougal, Initial velocity effect on space-charge-limited currents, *J. Appl. Phys.* **78**, 5919 (1995).
- [64] P. V. Akimov, H. Schamel, H. Kolinsky, A. Y. Ender, and V. I. Kuznetsov, The true nature of space-charge-limited currents in electron vacuum diodes: A Lagrangian revision with corrections, *Phys. Plasmas* **8**, 3788 (2001).
- [65] J. M. Halpern, A. M. Darr, N. R. S. Harsha, and A. L. Garner, A coordinate system invariant formulation for space-charge limited current with nonzero injection velocity, *Plasma Sources Sci. Technol.* **31**, 095002 (2022).
- [66] A. M. Loveless, A. M. Darr, and A. L. Garner, Linkage of electron emission and breakdown mechanism theories from quantum scales to Paschen’s law, *Phys. Plasmas* **28**, 042110 (2021).
- [67] R. E. Caffisch and M. S. Rosin, Beyond the Child-Langmuir limit, *Phys. Rev. E* **85**, 056408 (2012).
- [68] Y. Feng and J. P. Verboncoeur, Consistent solution for space-charge-limited current in the relativistic regime for monoenergetic initial velocities, *Phys. Plasmas* **15**, 112101 (2008).